

Generation of Photonic Crystal End Faces Using Laser Microfabrication

Thorsten SCHWEIZER¹, André NEUMEISTER¹, Qingchuan GUO¹, Wendel WOHLLEBEN², Reinhold J. LEYRER²,
Rainer KLING¹ and Andreas OSTENDORF¹

¹ Laser Zentrum Hannover e.V., Hollerithallee 8, 30419 Hannover, Germany

E-mail: t.schweizer@LZH.de, a.neumeister@LZH.de

² BASF Aktiengesellschaft, 67056 Ludwigshafen, Germany

We present a number of laser microfabrication methods to generate high quality end faces of photonic crystal templates. We have produced opal templates of 1 μm polystyrene spheres with 10-30 μm thickness on glass substrates using the self-assembly technique. In order to gain access to the useable area in the centre of the polystyrene opals, we modified the glass substrates and the opals with pulsed ns and ps UV lasers. By writing micro grooves into the substrate, changing the wettability of the substrates surface, and by using micro stereo lithography to fabricate polymer structures on top of the substrates, we generated good quality crystal end faces accessible for direct fibre coupling. The polymer structures allowed us to gain control of the crystal orientation. We also used a UV laser to make the glass substrates hydrophilic, which is a necessary prerequisite for the crystal growth process.

Keywords: Photonic crystal, polystyrene, micro stereo lithography, polymer, laser microfabrication, optical waveguides, surface modification, hydrophilic, pulsed lasers

1. Introduction

Materials that are periodically structured on a micrometer length scale in all three dimensions offer the possibility of obtaining a complete photonic band gap, a range of energy for which a photon cannot propagate in any direction inside the structure [1]. Such photonic crystals would allow us to manipulate the flow of light and are promising materials for photonic devices, which could find applications in areas such as telecommunications [2]. Our crystal structure of choice is the inverted opal structure, which can be fabricated from an opal template of polystyrene spheres. Whereas the polystyrene opal does not have a complete photonic band gap, the inverted opal made of a high refractive index material such as silicon does [3,4]. In section 2 we describe the fabrication of opal templates from polystyrene spheres, the first step in the production of photonic crystal devices.

The second step involves the generation of defects in the crystal structure, which locally close the band gap and thus allow the controlled propagation of light inside the photonic crystal. A line of defects acts as a waveguide for light within the forbidden wavelength range. We fabricated polymer defect waveguides using the two-photon polymerisation effect induced by femto-second laser pulses [5]. A description of this fabrication process will not be given in this paper but can be found in the literature [2,5,6]. The defect structures such as straight or bent waveguides have been inscribed in the central area of the polystyrene opal where the crystals have the highest homogeneity and thickness. In order to gain information about the quality, shape and size of the inscribed waveguides, we require access to the ends of the waveguides. This is a non-trivial engineering problem since both the delicate crystal and the substrate

need to be broken or cut to allow close access to the waveguides, for example for direct fibre coupling.

In this paper, we present a number of laser microfabrication methods to generate high quality crystal end faces in order to gain access to the inscribed waveguides (section 3.). For this purpose we pursue two different strategies. The first strategy is to prepare the glass substrates prior to crystal growth (section 3.1.), and the second strategy entails the treatment of substrates, which have already been covered with polystyrene opals (section 3.2.).

2. Fabrication of polystyrene opals

We have produced opal templates of about 1 μm polystyrene spheres with 10-30 μm thickness on 18x18 mm² cover glasses using the self-assembly technique [7]. The microscope slides are pre-treated in Piranha acid, making them superhydrophilic. Piranha acid, also known as Caro acid, is prepared by slowly mixing two parts of H₂SO₄ (96%) into one part of H₂O₂ (30%). The glass slides are immersed into the hot mixture and left there for a duration of up to 10 h. This preparation removes all organic matter and hydrophilizes the glass surface. Contact angles are below 10°. The slides are rinsed with water and then used as substrates for self-assembly. The self-assembly technique uses the deposition from a 0.3wt% diluted dispersion in ultra pure water onto an inclined substrate at 60° from horizontal by evaporation. The polymer dispersions are diluted without any further purification such as filtration and/or centrifugation and re-dispersion. The evaporation takes place at controlled 40±0.5°C and controlled 50% relative humidity. The particle diameter of 0.95 μm aims at the telecom wavelengths after inversion with silicon.

3. Generation of crystal end faces

Figure 1 illustrates the motivation for this paper. Please note that the figure is not drawn to scale. The thickness of the glass substrate is about 150 μm whereas the maximum thickness of the opal is only 10-30 μm . Polymer defect waveguides are inscribed into the useful area in the center of the polystyrene opal. The outer areas of the opal and the glass substrate prevent close access to the ends of the waveguide for inspection and characterisation.

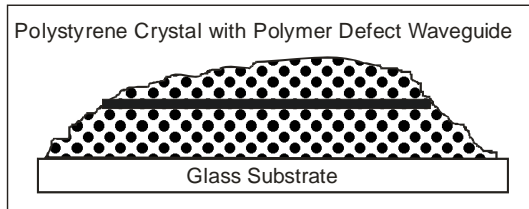


Fig. 1: Schematic of a polystyrene opal with an inscribed polymer defect waveguide on a cover glass substrate (not to scale)

In order to provide this access we performed some investigations about the generation of accessible high quality crystal end faces. Since the polystyrene opals act as a template for the final inverted opal structure, the quality of the end faces of the template will be transferred to the final device. The results of our investigations are presented in the following sections. The first section covers the treatment of the substrates before crystal growth (3.1.), while the second section considers the treatment of substrate and crystal after crystal growth (3.2.).

3.1. Treatment of the substrate before crystal growth

Prior to crystal growth we applied three different laser-based processes to the glass substrates: (i) cutting grooves into the substrate (3.1.1.), (ii) fabricating polymer structures on the substrates (3.1.2.), and (iii) modifying the surface of the substrate for selective adjustment of the surface wettability (3.1.3.). The results of combining these three laser-based processes will be presented in section 3.1.4.

3.1.1. Prescribing of glass substrates

The first treatment of the glass substrates prior to crystal growth is the fabrication of grooves across the whole width of the cover glasses. These grooves will aid defined breaking of substrate and crystal after crystal growth on the opposite side of the cover glass (figure 2).

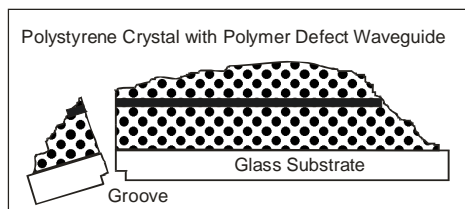


Fig. 2: Schematic of the generation of crystal end faces by prescribing and breaking of substrate and crystal (not to scale)

We compared two different laser sources, a frequency-quadrupled 30 ns Nd:YVO laser at 266 nm and an ArF excimer laser at 193 nm, and varied the process parameters

such as pulse energy and feed rate to find the optimum depth and shape of the grooves. Grooves with a depth of about 40 μm in the 150 μm thick glass substrates turned out to be the best compromise between defined breakability and sufficient stability for further processing of the substrates. Substrates with grooves of rectangular profile produced by the excimer laser turned out to be more resistant to breaking during the treatment with Piranha acid (see section 2.) than substrates with grooves of triangular profile produced by the Nd:YVO laser (see figure 5).

Figure 3 shows an example of a polystyrene opal after breaking. While the edge of the glass substrate is very smooth and straight, the end face of the crystal still displays some irregularities. Also, the crystal does not break parallel to the glass edge because the crystal axis is not aligned with the groove. Still, prescribing and breaking substrate and crystal is a step forward to an accessible crystal end face.

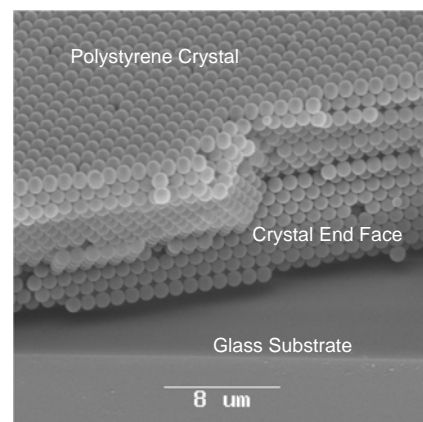


Fig. 3: Polystyrene crystal and glass substrate after breaking

3.1.2. Fabrication of polymer support structures on the substrates

The above results can be further improved by aligning the crystal axis with the grooves in the substrate. For this purpose, we used a micro stereo lithography setup [8] to fabricate polymer support structures that run parallel to the grooves on the opposite side of the substrate in order to force the crystal to grow parallel to the grooves. Figure 4 illustrates this idea.

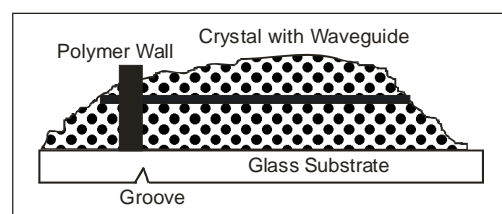


Fig. 4: Schematic of a polystyrene crystal grown on a substrate with a polymer wall and a groove (not to scale)

Figure 5 shows an SEM image of a pre-treated glass substrate with polymer wall and groove ready for the crystal growth process. After crystal growth on either side of the polymer wall the glass substrate can be broken along

the prescribed groove thereby generating a smooth and accessible crystal end face.

The polymer wall with a width of 200 μm and a height of 50 μm was fabricated by illuminating a film of a liquid photo-curable polymer (ORMOCER[®]) between two glass substrates separated by a 50 μm thick foil with a frequency-tripled 10 ps Nd:YAG laser at 355 nm. The laser beam is moved across the sample by using a scanner (Hurricane 14) and focused by a 100 mm F-Theta objective. After illumination, the non-polymerized ORMOCER[®] is removed by chemical treatment with a solution of isopropanol (two parts) and 4-methyl-2-phentanol (one part). Best quality walls were obtained with an average laser power of 100 μW , a hatch distance of 2 μm and a writing speed of 700 mm/s. The polymer walls were positioned precisely parallel and opposite to the grooves (see figure 5) by using an online observation system with a camera.

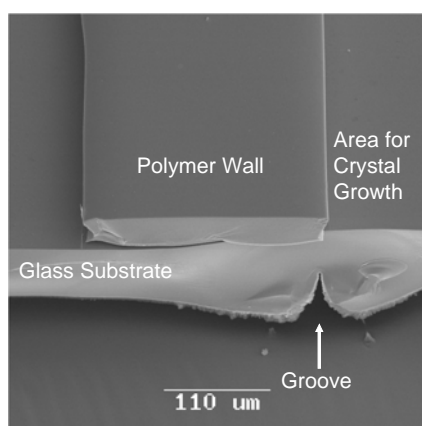


Fig. 5: Polymer wall on glass substrate with groove (viewing angle of 45°)

When we prepared the glass substrates with polymer walls for crystal growth, we noticed that the polymer walls were sensitive to the treatment with Piranha acid. As mentioned above, this treatment is a necessary preparation for the crystal growth process for which a hydrophilic surface is required (see section 2.). In order to avoid the destruction of the polymer walls by the Piranha acid, we substituted the acid treatment with a laser treatment. This process step will be explained in the next section 3.1.3.

3.1.3. Surface modification of the glass substrate

Since the polymer support structures are heavily affected by the treatment with Piranha acid (up to destruction), alternative routes have to be found for hydrophilisation of the glass substrates prior to crystal growth. Based on previous measurements, a contact angle $\theta < 20^\circ$ could be achieved using the Piranha acid (non-treated glass $\theta > 45^\circ$). It is well known from literature that focused laser radiation can be used to adjust selectively the wettability of technical surfaces [9]. Here, Gollapudi et al. have used a Nd:YVO laser to generate hydrophilic and hydrophobic surfaces on polymers like Polyimide (PI) or Polycarbonate (PC). In this presented work, an identical optical setup has been used for irradiation of the glass substrates, see [9] for details. The Nd:YVO laser operated at 30 kHz, and the 266-nm radiation was focussed by a 160-mm F-Theta objective. In a first

instance, glass surfaces have been selectively irradiated with a laser fluence ranging from $0.76 \text{ mJ/cm}^2 < H_{0,\text{Glass},Z_0} < 1.30 \text{ mJ/cm}^2$ (fluence in the focal position) in order to find a process parameter window. The samples have been processed in the focal plane (z_0) and at $z = -1 \text{ mm}$, -2 mm and -3 mm , respectively, by scanning vertically and horizontally arranged lines with a constant distance of $d_h = 25 \mu\text{m}$. The scanning velocity v_s has been 100 mm/s. The modified areas ($7 \times 7 \text{ mm}^2$ each) have been characterised using optical microscopy and scanning electron microscopy. Further, the contact angle θ of the generated surfaces has been determined using a Data Physics SCA20. It has been found during the investigations, that the final result strongly depends on the laser fluence H_{0,Glass,Z_0} and the sample position during processing (z). Figure 6 shows a modified surface which has been generated with $H_{0,\text{Glass},Z_0} = 1.02 \text{ mJ/cm}^2$ and $z = -2 \text{ mm}$ using an average laser power of 159 mW.

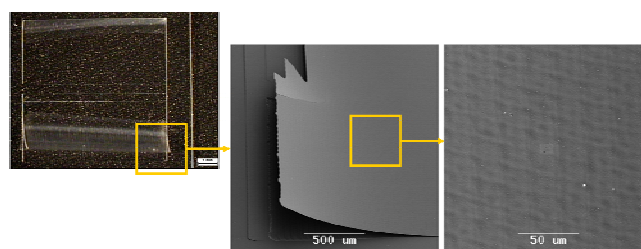


Fig. 6 (a) – (c): Microscope image of a laser processed area (a) and detailed SEM images (b, c), $H_{0,\text{Glass},Z_0} = 1.02 \text{ mJ/cm}^2$ and $z = -2 \text{ mm}$

As depicted, parts of the irradiated glass area detach from the original surface (figure 6 (a), (b)). On the other hand, a clear periodic structure has been induced on the surface of the glass substrate. No micro cracks or other damage due to ablation has been observed. Figure 7 shows a modified surface which has been generated with $H_{0,\text{Glass},Z_0} = 1.10 \text{ mJ/cm}^2$ and $z = -3 \text{ mm}$ using an average laser power of 161 mW.

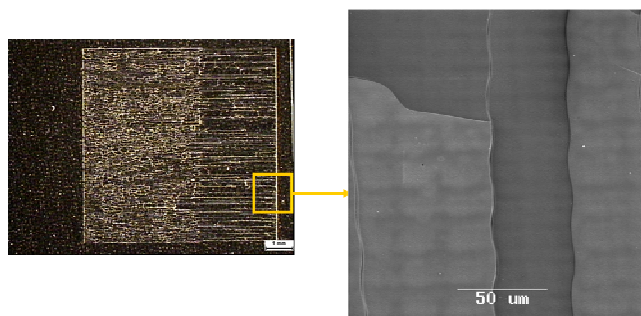


Fig. 7 (a), (b): Microscope image of a laser processed area (a) and detailed SEM image (b). The parameters have been $H_{0,\text{Glass},Z_0} = 1.10 \text{ mJ/cm}^2$ and $z = -3 \text{ mm}$

In contrast to the results shown in figure 6, various micro cracks have formed on the surface. Figure 8 is showing a detailed view of an SEM image. In contrast to the previously shown results, a periodic structure (similar to the one shown in figure 6) was fabricated. Here, no delaminations

of glass parts or micro cracks have been observed. The contact angle of the surface displayed in figure 8 has been measured using 3 μL of deionised water. The contact angle has been $\theta < 20^\circ$, which is in the range of the result achieved with the Piranha acid. This obtained result has been used during the course of our work.

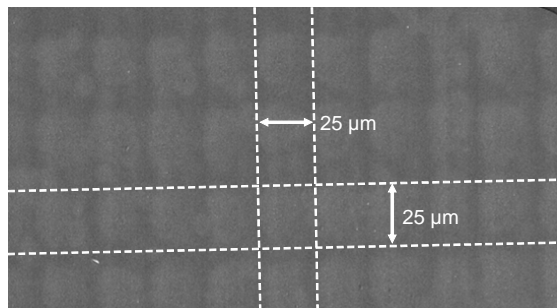


Fig. 8: Detailed view of an SEM image of a laser modified surface without damage or delaminations. The parameters have been $H_{0,Glass,Z_0} = 1.02 \text{ mJ/cm}^2$, $z = -3 \text{ mm}$ and $d_h = 25 \mu\text{m}$

In order to form both a polymer support structure and hydrophilic surface on one glass sample, the following procedure is proposed: Since the fabrication of polymer support structures involves chemical treatment of the substrate (see 3.1.2) that might influence the hydrophilic surface, the laser modification has been done after the fabrication of support structures. For this purpose, a slightly different approach has been followed for the production of the polymer support structures, mainly to achieve structures with higher aspect ratio. In contrast to the previously described method using a cavity with defined thickness of only 50 μm (3.1.2), we here used a cavity with a non-defined thickness of several mm (figure 9).

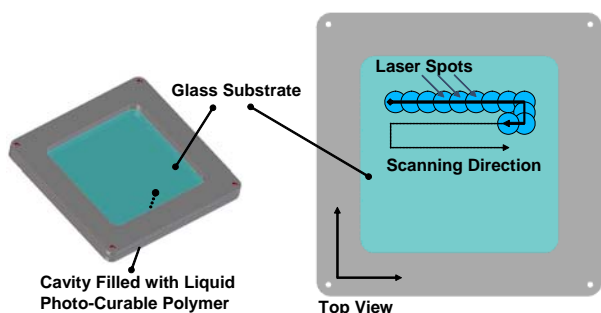


Fig. 9: Sketch of the applied setup for producing polymer support structures

In this way, the structures height was not limited by the thickness of the cavity, but only by the curing depth of the photo-curable material allowing the production of higher structures. The scanning principle remained identical to the method described in 3.1.2. The best result has been achieved with a laser power of $P_L = 300 \mu\text{W}$, a scanning velocity of $v_s = 50 \text{ mm/s}$ and a hatch distance of $d_h = 1 \mu\text{m}$. (figure 10). The height of the structure was around 180 μm at a width of 60 μm .

It has been shown that during the laser modification process of the glass surface, parts of the generated support structures are ablated. In this way, a periodic pattern develops on the surface of the support structure. On the other hand, a well-defined sharp edge develops at the side of the support structures (figure 11). The height of the structure was reduced from originally 180 μm to 17 – 60 μm .

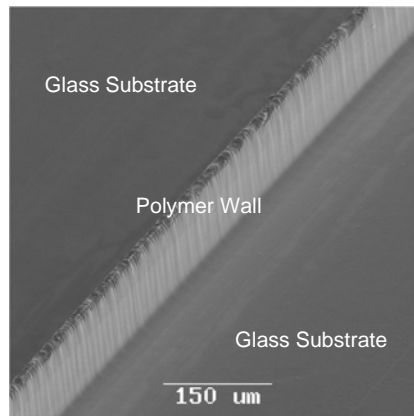


Fig. 10: SEM image of a polymer support structure generated with $P_L = 300 \mu\text{W}$, a scanning velocity of $v_s = 50 \text{ mm/s}$ and a hatch distance of $d_h = 1 \mu\text{m}$

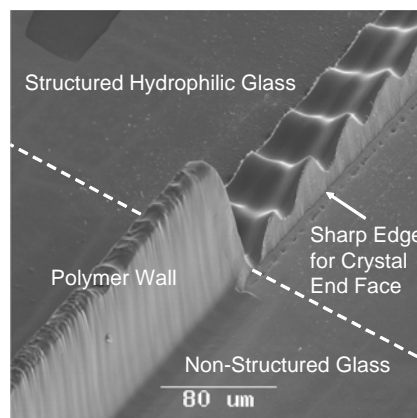


Fig. 11: SEM image of glass substrate with a polymer support structure on top. Indicated structured areas of the samples surface are hydrophilic ($\theta < 20^\circ$)

3.1.4. Results of combining polymer walls and surface modification

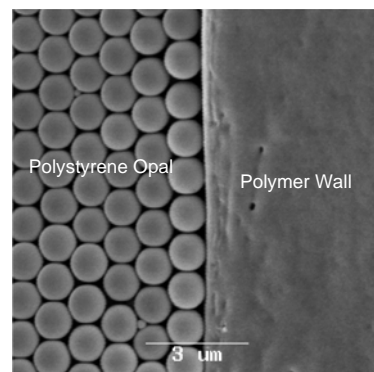


Fig. 12: SEM image of a polystyrene crystal near a polymer wall

We could successfully grow polystyrene crystals on laser-treated glass substrates with polymer walls. Figure 12 shows how the crystal structure is orientated along the polymer wall and hence the crystal axis will also be aligned with the groove at the backside of the glass substrate.

Figure 13 shows a polystyrene crystal end face after physically removing the polymer wall. The end face of the remaining polystyrene crystal possesses a largely improved quality when compared to merely breaking the substrate and crystal without support structures as shown in figure 3. Such a smooth crystal end face would allow close fibre coupling for inspection of the inscribed waveguides.

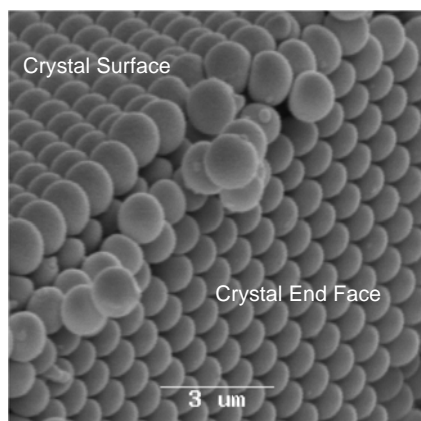


Fig. 13: SEM image of a polystyrene crystal end face after removal of the polymer wall.

As a next step, we will fabricate glass laser-treated substrates with both polymer walls and grooves, grow polystyrene opals on these substrates, and perform breaking experiments.

3.2. Treatment of substrate and crystal after crystal growth

The ideas explained so far all involved the treatment of the substrate prior to crystal growth. We now describe some experiments we performed on substrate and crystal after crystal growth.

Instead of fabricating polymer support structures on the glass substrate before crystal growth, such structures can also be fabricated after the polystyrene opal has been grown. The support structures can be written directly into the crystal, which has been infiltrated with a liquid polymer, with the same laser system described in 3.1.2. The remaining liquid polymer can subsequently be removed in an isopropanol bath. The support structures are expected to protect the delicate crystal during the breaking or cutting process.

As proof of principle, we infiltrated polystyrene crystals with ORMOCER[®] and polymerized the samples completely using an UV lamp. These samples were then either broken or cut with a filament saw.

Figure 14 shows the crystal end face after breaking a substrate and crystal. Due to the support from the polymer, the crystal breaks along the glass edge. Without polymer, the crystal tends to break away from the glass edge (figure 3). The smoothness of the crystal end face is acceptable for

inspection but not as good as the end face shown in figure 13.

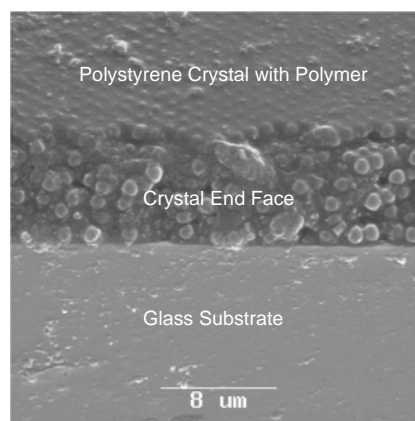


Fig. 14: SEM image of a completely infiltrated polystyrene crystal after breaking

Instead of breaking substrate and crystal, we also performed some cutting experiments. For these experiments, we used a filament saw (Meyer Burger RTS 440) with 200 μm thick steel wire with an electroplated 15 μm diamond grit. The filament moved at a speed of 500 m/min and slowly cut the sample with a feed rate of 5 $\mu\text{m}/\text{s}$. We cut the sample dry, without any cooling liquid. Figure 15 shows a crystal end face produced by this cutting process. The end face is smooth and runs parallel to the glass edge. As for the breaking process, the infiltrated polymer protects the crystal. Cutting experiments with a sample not protected by cured polymers led to a complete destruction of the crystal.

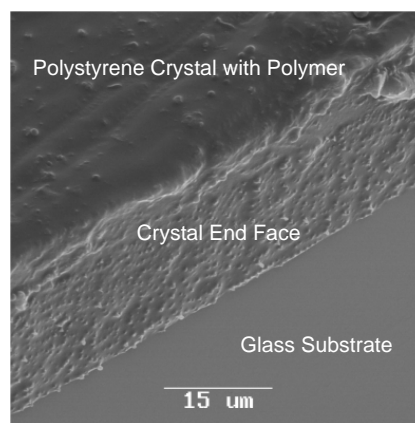


Fig. 15: SEM image of a completely infiltrated polystyrene crystal after cutting with a filament saw

For both the breaking and cutting experiments, we used completely infiltrated crystals. We will repeat these experiments using samples with locally defined support structures, which can be produced by the laser-based stereolithography process described in section 3.1.2.

4. Conclusion

We presented a number of laser-based microfabrication processes for the generation of accessible high quality end faces of photonic crystals. We used excimer and frequency

converted neodymium lasers to pre-treat the 150 μm thin glass substrates by cutting grooves into the substrate, fabricating polymer support structures on top of the substrate and by making the substrate hydrophilic before crystal growth. The combination of grooves that define the breaking of the crystal and polymer walls that define the crystal orientation, led to good quality crystal end faces parallel to the glass edge. In particular, by fabricating polymer structures on the substrate, we gained control of the orientation and alignment of the crystal, thereby opening up new possibilities to engineer photonic crystals.

We also showed how support structures written directly inside the crystal could improve the stability and alignment of the crystal in subsequent breaking and cutting experiments.

In the future, we will apply some of the presented methods to polystyrene templates with inscribed horizontal waveguides. In this way we will gain access to the ends of the waveguides, for example for direct fibre coupling. The quality of the crystal end face will be transferred to the final device after inversion of the polystyrene template.

Acknowledgements

This work has been supported in part by the European Commission (EC) 6th Framework Programme (FP6), under the (STREP) project NMP-4-CT-2005-017160 (NewTon), (www.projectnewton.com). We would like to thank Caspar Morsbach from Klein&Becker GmbH&CoKG for performing the cutting experiments with the filament saw.

References

- [1] E. Yablanovich: Phys. Rev. Lett., 55, (1987) 2059
- [2] P.V. Braun, S.A. Rinne and F. García-Santamaría: Adv. Mater., 18, (2006) 2665.
- [3] A. Blanco, E. Chomski, S. Grabtchak, M. Ibisate, S. John, S.W. Leonard, C. Lopez, F. Meseguer, H. Miguez, J.P. Mondia, G.A. Ozin, O. Toader and H.M. van Driel, Nature, 405, (2000) 437
- [4] Y.A. Vlasov, X.-Z. Bo, J.C. Sturm and D.J. Norris, Nature, 414, (2001) 289
- [5] M. Boyle, A. Neumeister, J. Zinn, W. Wohlleben and R.J. Leyrer, Proc. SPIE, (2008) 6901
- [6] Y. Jun, C.A. Leatherdale and D.J. Norris, Adv. Mater., 17, (2005) 1908
- [7] W. Wohlleben, F. W. Bartels, S. Altmann and R. J. Leyrer: Langmuir, 23, (2007) 2961
- [8] A. Neumeister, R. Himmelhuber, C. Materlik, T. Temme, F. Pape, H.-H. Gatzert and A. Ostendorf, JLMN, 3, (2008) 67
- [9] S. Gollapudi, F. Otte, T. Temme, U. Stute, Proc. of 6th LPM (2005)

(Received: June 16, 2008, Accepted: October 28, 2008)